ACS APPLIED MATERIALS & INTERFACES

Research Article

www.acsami.org

Interfacial Tension Effect on Cell Partition in Aqueous Two-Phase Systems

Ehsan Atefi,[†] Ramila Joshi,[†] Jay Adin Mann, Jr.,[‡] and Hossein Tavana*[,†]

[†]Department of Biomedical Engineering, The University of Akron, Akron, Ohio 44325, United States

[‡]Department of Chemical and Biomolecular Engineering, Case Western Reserve University, Cleveland, Ohio 44106, United States

Supporting Information

ABSTRACT: Aqueous two-phase systems (ATPS) provide a mild environment for the partition and separation of cells. We report a combined experimental and theoretical study on the effect of interfacial tension of polymeric ATPS on the partitioning of cells between two phases and their interface. Two-phase systems are generated using polyethylene glycol and dextran of specific properties as phase-forming polymers and culture media as the solvent component. Ultralow interfacial tensions of the solutions are precisely measured using an axisymmetric drop shape analysis method. Partition experiments show that two-phase systems with an interfacial tension of 30 $\mu J/m^2$ result in distribution of majority of cells to the bottom dextran phase. An increase in the interfacial tension results in a distribution of cells toward the interface. An independent cancer cell spheroid formation assay confirms these observations: a drop of the dextran phase containing cancer cells is dispensed into the immersion polyethylene glycol phase to form a cell-containing drop. Only at very small interfacial tensions do cells remain within the drop to aggregate into a spheroid. We perform a thermodynamic modeling of cell partition to determine variations of free energy associated with displacement of cells in ATPS with respect to the ultralow interfacial tensions. This modeling corroborates with the experimental results and demonstrates that at the smallest interfacial tension of 30 $\mu J/m^2$, the free energy is a minimum with cells in the bottom phase. Increasing the interfacial tension shifts the minimum energy and partition of cells toward the interfacial region of the two aqueous phases. Examining differences in the partition behavior and minimum free energy modeling of A431.H9 cancer cells and mouse embryonic stem cells shows that the surface properties of cells further modulate partition in ATPS. This combined approach provides a fundamental understanding of interfacial tension role on cell partition in ATPS and a framework for future studies.

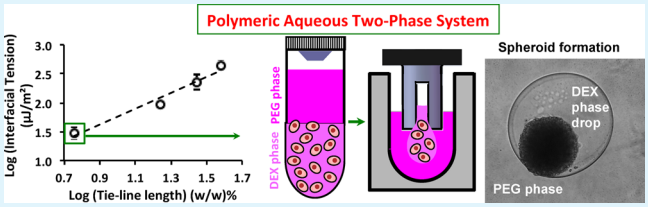

KEYWORDS: *cell partition, aqueous two-phase system, interfacial tension, thermodynamic model, cancer cells, embryonic stem cells*

INTRODUCTION

A polymeric aqueous two-phase system (ATPS) may form by dissolving two different polymers, for example, polyethylene glycol (PEG) and dextran (DEX), each above a certain concentration, in an aqueous medium. Phase separation takes place if interactions between like polymer molecules are energetically more favorable compared to interactions between molecules of two different polymers used for ATPS formation.[1] A large number of polymers can form ATPS; PEG and DEX are widely used in the context of biological and bioprocesses applications. Each equilibrated aqueous phase from an ATPS is enriched with respect to one of the polymers.[1] For example in an ATPS formed with aqueous PEG and DEX solutions, the top phase is enriched with PEG, whereas the bottom phase contains majority of DEX.

ATPS are widely used for fractionation and partition of biomolecules including proteins,[2−4] subcellular organelles and plasma membranes,[5,6] bacterial,[7−9] viral,[10−12] and mammalian cells,[13,14] as well as small and large particles.[15,16] ATPS provide a mild and highly aqueous environment to maintain activities and functions of biomolecules. Polymers such as polyethylene glycol used for ATPS formation also provide additional protective effect for biomolecules.[17] Each ATPS is characterized by a specific phase diagram that shows the range of concentrations of phase-forming polymers to produce two immiscible aqueous phases and gives the composition of equilibrated phases (Figure SI-1).

Controlling partition of cells in ATPS has recently enabled novel cell patterning and printing approaches for tissue engineering applications. These methods primarily use PEG and DEX as phase-forming polymers and rely on selective partition of cells to one of the aqueous phases or the interface between them. Dispensing a drop of the aqueous DEX phase containing stem cells onto a layer of adhered stromal cells immersed in the aqueous PEG phase created cocultures that led to differentiation of stem cells to neurons.[18,19] In a different application, dispensing discrete drops of the DEX phase containing cancer cells into a nonadherent microwell containing the immersion PEG phase resulted in aggregation of cells into a three-dimensional cluster known as a cellular

Received: June 27, 2015
Accepted: September 10, 2015
Published: September 10, 2015

DOI: 10.1021/acsami.5b05757
ACS Appl. Mater. Interfaces 2015, 7, 21305−21314

spheroid.[20,21] Complete exclusion of cancer cells from aqueous DEX phase drops printed on a culture plate, or in other words complete partition of cells to the immersion PEG phase, generated a monolayer of cells containing a circular cell-excluded gap that served as the migration niche for adhered cells.[22−24] Selective partition of cells to the interface of two aqueous phases allowed a straightforward method of creating skinlike constructs.[25] In all these applications, effective partition of cells to a desired phase of the ATPS or the interface was critical.

Partition of large particles such as cells in an ATPS depends on surface properties of particles and physical properties of the two-phase system.[26] Surface area, surface charge, and wettability of surface of cells, ionic composition, pH, and temperature of separation medium, molecular weight of polymers, and interfacial tension between the two aqueous phases are important parameters that influence cell partition in ATPS. We herein report a study of interfacial properties of two-phase solutions from a specific ATPS that lead to fractionation of cell particles and help evaluate the effect of interfacial tension on cell partition. Major challenges are the difficulty of reproducible measurements of *ultralow* interfacial tensions of ATPS, that is, $\gamma_{l_1l_2} \ll 1$ mJ/m^2, and measurements of contact angles of cell particles at the interface of immiscible aqueous solutions used as a tool to probe surface properties of cells.

We exploit a drop shape methodology to precisely determine ultralow interfacial tensions of ATPS.[27] A pendant drop of the aqueous DEX phase is formed in the immersion PEG phase and allowed to autonomously dispense. Images of the growing drop are captured, and drop profiles are extracted using image processing techniques (see the inset in Figure 1 for an example

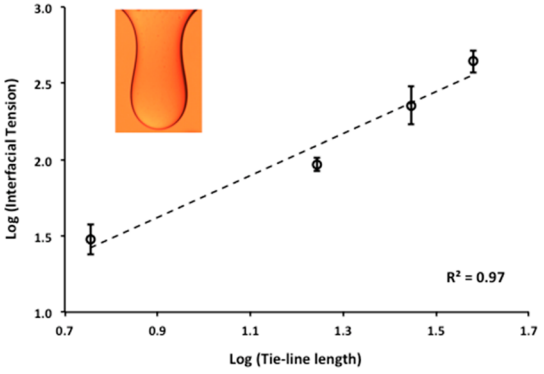

Figure 1. Ultralow interfacial tensions, in microjoules per square meter, of four two-phase systems made with different concentrations of PEG and DEX are shown against tie-line length, in weight percent, on a logarithmic scale (base 10). Dashed line is a fitted line to data, and R^2 shows the goodness of the fit. Tie-line lengths for these systems are given in Table 1. (inset) A well-deformed pendant drop from an experiment for interfacial measurement with the 10.0% PEG−12.8% DEX system.

of the drop images analyzed). The shape of the drop is governed by the Laplace equation;[28] hence, Laplacian curves are numerically fitted to the extracted profiles. The best fit that satisfies specific criteria for a well-deformed drop returns the interfacial tension between the DEX phase drop and the PEG phase. In addition, we characterize the complex cell-ATPS interface through measurements of the contact angles that the interface makes with cell particles, using an accurate technique based on polynomial fitting to the cell-ATPS interface.[29]

We show that partition of cells in ATPS generated with PEG and DEX of specific properties is sensitive to changes in the interfacial tension when other factors such as composition of the solvent (culture media), temperature, pH, and polymer properties are kept fixed. Independent partition experiments and a spheroid formation assay confirm that a very small interfacial tension is required to partition cells to the aqueous DEX phase. We complement our empirical work with a theoretical modeling of free energy of displacing cell particles in a two-phase system and demonstrate that a very low interfacial tension correlates with a minimum energy when cells locate in the bottom DEX phase. Increasing the interfacial tension shifts the minimum energy state and favors distribution of cell particles toward the interface. Importantly, this model incorporates measured quantities of interfacial tensions of ATPS and contact angles at ATPS−cell interface to predict distribution of cell particles between two aqueous phases and their interface. We believe that our experimental−theoretical study provides a new approach to understand cell partition in ATPS.

EXPERIMENTAL SECTION

Preparation of Aqueous Two-Phase Systems. Polyethylene glycol (PEG) with a molecular weight of 35 kDa (Sigma) and dextran (DEX) with a molecular weight of 500 kDa (Pharmacosmos) were used for ATPS formation. Four different sets of two-phase systems were formed using 5.0% PEG−6.4% DEX, 10.0% PEG−12.8% DEX, 15.0% PEG−19.2% DEX, and 25.0% PEG−25.6% DEX. Polymers were received in a powder form. Concentrations of aqueous PEG and DEX solutions were calculated in %(w/v). Both polymers were dissolved in complete growth media described below. To facilitate dissolution of polymers, solutions were kept in a 37 °C water bath for ∼1 h while vortexing them for 2 min every 10 min.[30]

Constructing Binodal Curve. A titration method was implemented to construct an experimental binodal curve for the ATPS with PEG and DEX as phase-forming polymers.[31] Two-phase solutions over a wide range of concentrations were prepared in 1.5 mL microcentrifuge tubes and weighed. Next, distilled water was added dropwise to each solution until the segregation line between top PEG phase and bottom DEX phase disappeared. Concentrations of polymers in each two-phase solution just prior to transition to a single-phase solution produced one point on the binodal curve. Binodal curve was constructed by curve fitting to experimental data points.[20] Length of tie-lines of two-phase systems were calculated using concentrations of PEG and DEX in top and bottom equilibrated phases.

Preparation of Suspensions of Cells. A431.H9 human skin cancer cells were kindly provided by Dr. Mitchel Ho (Center for Cancer Research, NIH, Bethesda, MD) and cultured in a complete growth medium composed of 88% Dulbecco's Modified Eagle's Medium (DMEM, Sigma), 10% fetal bovine serum (FBS, Sigma), 1% glutamine (Life Technologies), and 1% antibiotic (Life Technologies). Every 10 passage, cells were treated with 700 μg/mL of G418 (Sigma-Aldrich). T75 culture flasks were kept in a humidified incubator with 5% CO_2 at 37 °C to allow cells to form a monolayer of 80−90% confluent. Cells were dislodged with 2 mL of trypsin for 2 min. Trypsin was neutralized by adding 4 mL of growth medium. Mouse embryonic stem cells (mESCs) were purchased from Riken and maintained on 0.1% gelatin-coated 35 mm Petri dishes at 37 °C in a humidified incubator with 5% CO_2. mESCs were cultured in Glasgow Minimum Essential Medium (GMEM, Life Technologies) supplemented with 1% FBS, 10% knockout serum replacement (KSR, Life Technologies), 2 mM glutaMAX (Life Technologies), 0.1 mM nonessential amino acids (NEAA, Life Technologies), 1 mM sodium pyruvate (Life Technologies), 0.1 mM 2-mercaptoethanol (Life Technologies), and 2000 U/mL leukemia inhibitory factor (Millipore). mESCs were dislodged with 1 mL of trypsin-EDTA for 1 min. Trypsin was neutralized by adding 3 mL of growth medium. Both

DOI: 10.1021/acsami.5b05757
ACS Appl. Mater. Interfaces 2015, 7, 21305−21314

A431.H9 cell and mESC suspensions were centrifuged at 1000 rpm for 5 min. The supernatant was removed, and the cell pellet was resuspended in 1 mL of medium. The number of cells was counted using a hemocytometer.

Cell Partition in Aqueous Two-Phase Systems. With each cell type (A431.H9 and mESCs), cell suspensions were made by mixing ~6 × 10^6 cells with two-phase solutions consisting of 500 μL from each of PEG and DEX phases. All four sets of two-phase systems with different PEG and DEX concentrations were separately used. The conical was maintained vertically in an incubator with 5% CO_2 in 37 °C until two separate phases were formed. Volumes of top and bottom equilibrated phases were measured using graduations on the conical tube. Next, samples were taken from top and bottom phases and the interface and transferred into three separate microcentrifuge tubes. First, a pipet was set at 150 μL, the plunger button was depressed in air to its first stop, the pipet tip was moved into the top phase, and 150 μL was slowly aspirated from the middle of top phase. This was followed by taking a sample from the bottom phase. The pipet was set at 150 μL, and the plunger button was pushed to its second stop in air. Then the pipet tip was slowly moved through the top phase and the interface into the bottom phase while maintaining pressure on the plunger button to prevent liquid from entering into the pipet tip during its travel. The interface was quickly stabilized around the pipet tip. With the pipet tip in the middle of the bottom phase, the sample was aspirated by slowly releasing the plunger. After gently retracting the pipet tip from the conical tube, its exterior was blotted to remove solution residues. Slow movement of the pipet tip through the interface was crucial to avoid disturbing it. Using a similar approach, a sample was taken from the interface. The pipet tip was carefully brought in contact with the interface, and the plunger was slowly released to remove the solution from the interface. While maintaining a positive pressure on the plunger button, the pipet tip was moved out of the tube, and its exterior was blotted. Each of the three samples was diluted in in the growth medium 3 to 5 times by volume to make loading the suspension onto hemocytometer and counting of cells feasible. Diluted samples of each phase were separately loaded onto a hemocytometer, the number of cells was counted, and an average was calculated from four replicates. The total number of cells partitioned to each phase was determined by multiplying the average number of counted cells in that phase, volume of the equilibrated phase, a constant number 1 × 10^4, and a dilution factor. The number of cells partitioned to the interface was also calculated by subtracting the number of cells partitioned to top and bottom phases from the total number of cells used for the experiment.

Interfacial Tension Measurements. The ultralow interfacial tension between equilibrated top and bottom phases of each of four two-phase systems was measured using an axisymmetric drop shape analysis (ADSA).[27] A 2.5 μL glass syringe (Hamilton) was loaded with the DEX phase solution, connected to a 19-gauge needle, and held vertically on a micropositioning unit. The unit was assembled on a vertical rod fixed on an optical table from the bottom end. Using an X−Y translational control knob of the unit, the needle was lowered and gradually inserted into a rectangular glass cuvette (Helma) containing 1 mL of the aqueous PEG phase. The DEX phase solution autonomously dispensed and formed a growing pendant drop at the needle tip. Images of the growing drop were captured at 10 fps for 10 s. A Canny edge operator was used to extract the set of numbers that represent the drop profile. The interfacial tension was determined by finding a best Laplacian fit to the extracted drop profile.[28] For each two-phase system, an average interfacial tension was determined from five measurements, and the uncertainty was estimated.

Contact Angle Measurements. An 18 × 18 mm^2 microscopic glass slide was UV sterilized for 30 min. Each glass slide was placed in 35 mm Petri dish containing 4 mL of 0.5% aqueous gelatin solution (Sigma-Aldrich). After 3 h of incubation at 37 °C and 5% CO_2, the gelatin solution was removed, and 4 mL of cell suspension containing 3 × 10^4 cancer cells or 2 × 10^6 mESCs was added to the dish. To ensure formation of a uniform cell monolayer, glass slides with A431.H9 cancer cells were incubated for 24−36 h to allow cells to spread and grow. A shorter incubation time of 6 h was used for mESCs to prevent their differentiation, while the selected density allowed covering the slides with cells. After the culture medium was removed, glass slides containing the cell monolayer were washed with PBS three times and transferred into a glass cell (White Bear Photonics) filled with pre-equilibrated top phase from the desired two-phase system. A 0.7 μL drop of pre-equilibrated bottom phase of the same two-phase system was gently dispensed onto the slide using a pipet. The glass cell was incubated for 60 min at 37 °C and 5% CO_2. A camera (JAI Ltd., CB-200GE)-lens (LEICA, Z16 APO) unit assembled on an optical table was used to capture images of drops at a 9.2× magnification. Contact angles were measured using an automated polynomial fitting technique developed previously.[29] Each condition had five replicates.

Density Measurements. Densities of equilibrated phases from each two-phase system were measured using a density meter (Mettler Toledo, DA-100M) accurate to 0.001 gr/cm^3. A syringe loaded with 2 mL from each equilibrated phase was used to inject the solution into the glass measuring cell of the density meter. Prior to each round of measurement, the glass measuring cell was flushed with 20 mL of distilled water and 10 mL of ethanol and purged with a built-in pump. All measurements were done in a laboratory temperature of 24 ± 1 °C.

Spheroid Formation Assay. Aqueous PEG phase solutions were prepared in the complete growth medium at 5.0%, 10.0%, 15.0%, and 20.0% (w/v) and loaded into wells of a round-bottom, noncell-adherent 96-well plate. Aqueous DEX phase solutions were prepared at 12.8%, 25.6% DEX, 38.4% DEX, and 51.2% (w/v). A suspension of A431.H9 cells was prepared at a density of 25 × 10^3 cells/μL and thoroughly mixed with an equal volume of each of the DEX phase solutions. This reduced DEX concentration in each suspension in half to those used in cell partition experiments. A 0.3 μL drop of the resulting suspension was dispensed into each well. The dispensed drop contained 7.5 × 10^3 cells. Plates were incubated for 24 h, and spheroid formation was evaluated by phase contrast imaging of wells. For evaluating consistency of spheroid formation in a 96-well plate, DEX drops contained 15 × 10^3 cells and were dispensed using a robotic liquid handler (SRT Bravo, Agilent Technologies).[30] Spheroids were imaged using an inverted fluorescent microscope (Axio Observer A1, Zeiss) equipped with a high-resolution camera (AxioCam MRm, Zeiss).

RESULTS AND DISCUSSION

Interfacial Tensions of Aqueous Two-Phase Systems. After equilibration of each two-phase system, we separated top and bottom phases and used a pendant drop approach in ADSA to measure the interfacial tension between a DEX phase drop immersed in the PEG phase.[27] Measurements were done with all four two-phase solutions made with increasing concentrations of PEG and DEX. In addition, concentrations of PEG and DEX in equilibrated phases of each two-phase solution were determined from the phase diagram of the ATPS shown in Figure SI-1. Then, a tie-line length (TLL) was calculated for each two-phase system as[27]

$$\mathrm{TLL} = \sqrt{(C_{\mathrm{PEG,T}} - C_{\mathrm{PEG,B}})^2 + (C_{\mathrm{DEX,T}} - C_{\mathrm{DEX,B}})^2} \quad (1)$$

Here, $C_{PEG,T}$ and $C_{PEG,B}$ represent PEG concentration in top and bottom phases, and $C_{DEX,T}$ and $C_{DEX,B}$ denote DEX concentration in top and bottom phases, respectively. Figure 1 shows interfacial tensions of all four systems. Consistent with previous reports, interfacial tension increases linearly with the TLL on a logarithmic scale. TLL and interfacial tensions for each of the four two-phase systems used in this study are given in Table 1.

Partition of Cells in Aqueous Two-Phase Systems. We conducted systematic cell partition experiments using two different types of cells, namely, A431.H9 human skin cancer cells and mouse embryonic stem cells (mESCs), in two-phase solutions of four different interfacial tensions (Figure 1).

DOI: 10.1021/acsami.5b05757
ACS Appl. Mater. Interfaces 2015, 7, 21305−21314

Table 1. Phase Properties of Two-Phase Solutions[a]

system	PEG %(w/v)	DEX %(w/v)	TLL %(w/w)	$\gamma_{L_1L_2}$ (μJ/m^2)	$\rho_{\text{PEG phase}}$ (g/cm^3)	$\rho_{\text{DEX phase}}$ (g/cm^3)
1	5.0	6.4	5.7	30 ± 4	1.008	1.026
2	10.0	12.8	17.5	93 ± 6	1.012	1.062
3	15.0	19.2	27.9	226 ± 5	1.018	1.093
4	20.0	25.6	38.0	440 ± 5	1.027	1.125

[a]Tie-line length, interfacial tension of aqueous phases of four two-phase systems made with different weight fractions of PEG, Mw: 35 kDa, and DEX, Mw: 500 kDa, and measured densities of aqueous phases from each system are given.

Cancer cells and embryonic stem cells have substantially different gene and protein expression profiles, including membrane proteins,[32−36] that may reflect effects of cell surface properties on partition behavior of cells. A defined number of A431.H9 cells or mESCs (6×10^3 cells/μL) was included in each of the four systems. The conical tube containing ATPS and cells was inverted many times to produce a well-mixed suspension. The tube was incubated while being maintained vertical. After two immiscible phases formed, samples were removed from top and bottom phases and the interface (Figure 2a), and the number of cells in each sample was counted using a hemocytometer (Figure 2b). A partition coefficient was defined as the number of cells in the bottom phase divided by the total number of cells. We note that the selected cell density was based on preliminary experiments and ensured that cells would not clump into large aggregates during the partition process. Our analysis below shows that at a single cell level, the effect of gravity on cell partition is negligible.

With A431.H9 cells (Figure 2c), the two-phase system with the smallest interfacial tension of $\gamma_{l_1l_2}$ = 30 μJ/m^2 gave a large partition coefficient of 88 ± 5%. The remaining 12% of cells were primarily recovered from the top phase sample. Increase in the interfacial tension to $\gamma_{l_1l_2}$ = 93 μJ/m^2 in the second system significantly diminished cell partition to the bottom phase, resulting in a decrease of the partition coefficient to 34 ± 3%. This was accompanied by a large increase in the number of cells partitioned to the interface from 2 ± 1% in the first system to 47 ± 5% in the second system. The number of cells recovered from the top phase also showed a slight increase to 20 ± 6% in this system. Further increase in the interfacial tension to $\gamma_{l_1l_2}$ = 440 μJ/m^2 reduced the partition coefficient to 24 ± 4% and caused a moderate increase in cell partition to the

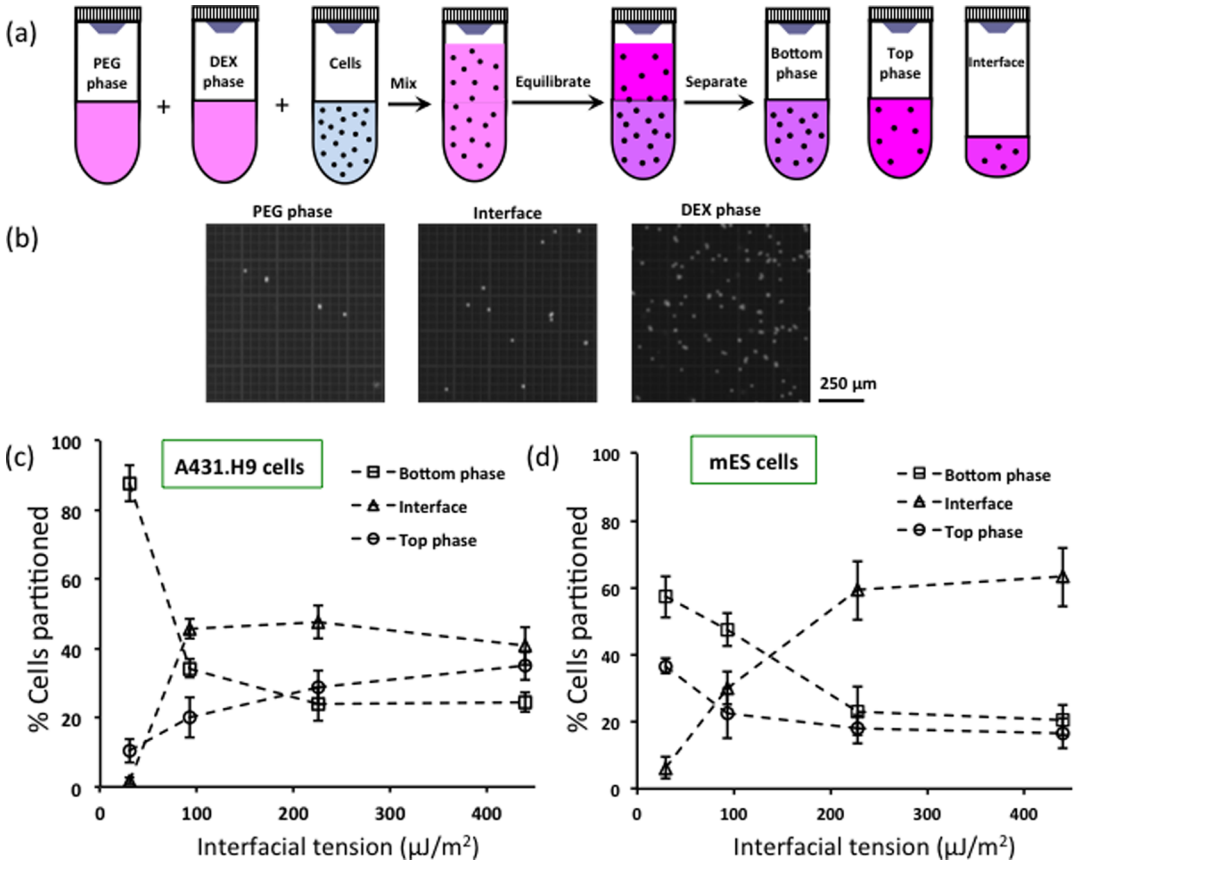

Figure 2. (a) Schematic of cell partition experiments with aqueous two-phase systems, (b) images of A431.H9 cells recovered from top phase, interface, and bottom phase of the 5.0% PEG−6.4% DEX two-phase system and loaded on a hemocytometer for counting, (c) percent of A431.H9 cells partitioned to each of the two bulk phases and their interface in four two-phase systems is shown vs interfacial tension. With the ATPS of lowest interfacial tension of $\gamma_{l_1l_2}$ = 30 μJ/m^2, cells primarily partition to the bottom DEX phase, resulting in a partition coefficient of 88 ± 5%. Increase in the interfacial tension to $\gamma_{l_1l_2}$ = 93 μJ/m^2 and above significantly changes distribution of cells toward the interface and the top PEG phase; (d) percent of mESCs partitioned to the PEG and DEX phases and their interface in four two-phase systems is shown vs interfacial tension. The largest partition coefficient of 58 ± 6% is obtained with the system of $\gamma_{l_1l_2}$ = 30 μJ/m^2. Increase in the interfacial tension distributes ∼60% of mESCs to the interface. Dashed lines are only used to connect data points.

DOI: 10.1021/acsami.5b05757
ACS Appl. Mater. Interfaces 2015, 7, 21305−21314

top phase to 35 ± 3%, whereas cell partition to the interface remained statistically unaltered.

With mESCs (Figure 2d), the largest partition coefficient was 58 ± 6% and obtained with the system of smallest interfacial tension of $\gamma_{l_1l_2}$ = 30 μJ/m^2. Majority of the remaining cells, that is, 37 ± 2%, partitioned to the top phase. The partition coefficient in the second system with $\gamma_{l_1l_2}$ = 93 μJ/m^2 dropped only 10% compared to the first system; more cells were found at the interface, and the number of cells in the top phase reduced to 22 ± 8%. A major decrease in the partition coefficient to 23 ± 7% was observed with the system of $\gamma_{l_1l_2}$ = 226 μJ/m^2. This was associated with a significant increase in the number of cells at the interface, that is, 59 ± 9%. Increase in $\gamma_{l_1l_2}$ to 440 μJ/m^2 gave the smallest partition coefficient of 20 ± 5% and the largest number of cells at the interface.

Two major conclusions emerge from these results. First, regardless of cell type used, the largest partition coefficient results from the two-phase system of smallest interfacial tension. However, there is a significant difference of 30% in the partition coefficient of cancer cells and mESCs in the system of $\gamma_{l_1l_2}$ = 30 μJ/m^2. This indicates that in addition to interfacial tension, properties of cells have a major effect on their partition in ATPS. Second, results from experiments with both cell types show a sharp drop in the partition coefficient (cf. Figure 2c,d). With mESCs, this occurs at a larger interfacial tension, that is, from system 2 to system 3, compared to A431.H9 cells. We will provide an explanation for these observations using thermodynamic modeling of cell partition that incorporates measured surface properties of cells. Overall, this study establishes the influence of ultralow interfacial tensions of polymeric ATPS on partition of cells between the two phases and their interface when properties of ATPS such as molecular weight of polymers, temperature, and pH of the separation medium are kept fixed.

Effect of Gravity on Cell Partition in Aqueous Two-Phase Systems. A partition experiment is initiated by inverting a conical tube containing ATPS and cells until a turbid, well-mixed suspension is formed. The resulting suspension contains small drops of one phase dispersed in the bulk of the second phase surrounding it, that is, drops of DEX phase in the PEG phase and vice versa.[1] Because of random motions within the solution, floating cells attach to these drops during the partition process (Figure 3).[1,37] Therefore, each cell particle experiences an interfacial force and a vertical force resulting from a balance between buoyant and gravitational forces. For the two-phase systems with $\gamma_{l_1l_2}$ = 0.03−0.44 dyn/cm studied here (Table 1), the interfacial force, $F_{int} = \gamma_{l_1l_2} A = \gamma_{l_1l_2} (2\pi r)$, is on the scale from 1 × 10^{-5} to 1 × 10^{-4} dynes, assuming a contact radius of r = 5 μm between the cell particle and the ATPS interface.

To determine the balance of buoyant and gravitational forces, $F = (\rho_P - \rho_f)V_P g = \Delta\rho V_P g$, we measured the density of aqueous phases of these four systems (Table 1) and used measured density of cells based on existing literature ($\rho_P \cong$ 1.1 g/cm^3)[38,39] and an approximate radius of 10 μm for cells based on measurements of volume of cells.[40] The largest downward vertical force is obtained with the first two-phase system ($\rho_f = \rho_{PEG}$ = 1.008 g/cm^3) that gives the largest density difference between a cell particle and the aqueous phase, that is, $\Delta\rho$ = 0.092 g/cm^3. This force is on the scale of $F \approx 4 \times 10^{-7}$ dynes. With measured densities for other aqueous phases in Table 1, this force becomes smaller and even negative (i.e., an upward force, e.g., considering $\rho_f = \rho_{DEX}$ = 1.125 g/cm^3 of system 4). Therefore, the vertical force acting on the particle is several orders of magnitude smaller than the interfacial force on the particle and comparatively negligible in the partition process. This analysis shows that gravity does not influence partition of cells in the two-phase systems studied here.

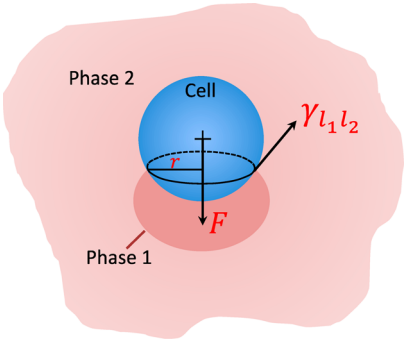

Figure 3. After inverting the conical tube containing ATPS and cells to initiate the partition process, small drops of one of the aqueous phases form within the surrounding second phase. These drops attach to the floating cell particles. The balance of interfacial force resulting from the interface between the cell and the ATPS interface ($F_{int} = \gamma_{l_1l_2} A = \gamma_{l_1l_2}(2\pi r)$), and net force due to buoyancy and gravity ($F = (\rho_P - \rho_f) V_P g = \Delta\rho V_P g$) shows that gravity effect is negligible on cell partition in ATPS.

It is important to note that the partition process is rather short and that samples are taken after a clear interface forms.[1] Allowing the phases to settle for too long may cause cells suspended in the top phase to form a sediment at the interface since cell density ($\rho_P \cong$ 1.1 g/cm^3) is larger than the density of the PEG phase in all four systems shown in Table 1.

Spheroid Formation in Aqueous Two-Phase Systems. Three-dimensional cultures of cancer cells have recently gained increasing interest in cancer research. Spheroids are three-dimensional clusters of cancer cells that mimic various properties of solid tumors and present a relevant tumor model for drug discovery.[41−43] To demonstrate the role of partition of cells on spheroid formation with ATPS, we performed a spheroid assay using all four systems made with the PEG 35k−DEX 500k ATPS. A suspension of A431.H9 cells was generated, and a drop of this suspension was dispensed into a microwell containing the PEG phase solution. Because of its higher density, the drop settled at the bottom of the microwell while remaining phase-separated from the immersion PEG phase. Our experience shows that A431 cells can form a compact spheroid within 24 h of incubation.[20] Therefore, we evaluated spheroid formation with all four two-phase solutions after 24 h. Figure 4a shows that the first system produced a compact spheroid within the DEX phase drop. By increase in the interfacial tension for other systems, cells only formed several small, loose aggregates close to the interface of the drop (Figure 4b). This test validates that with the system of the smallest interfacial tension studied here, cells primarily remain in the DEX phase drop to form a spheroid. However, the propensity of cells to partition to the interface and top phase in the other three systems disrupts self-assembly of cells into a spheroid. We confirmed that the 5.0% PEG−6.4% DEX system reproducibly generates uniformly sized spheroids. With a density of 15 × 10^3 cells, spheroids formed in a 96-well plate measured 391 ± 32 μm in diameter (Figure 4c). Therefore,

DOI: 10.1021/acsami.5b05757
ACS Appl. Mater. Interfaces 2015, 7, 21305−21314

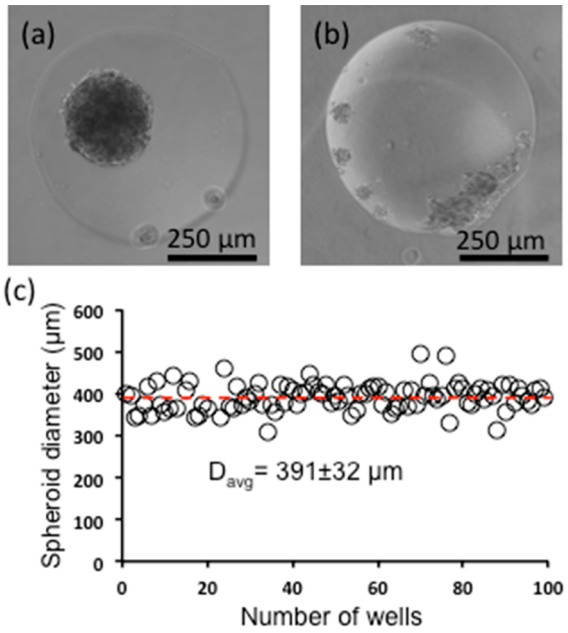

Figure 4. Spheroid formation assay performed with two-phase systems made with (a) 5.0% PEG−6.4% DEX and (b) 10.0% PEG−12.8% DEX. The first system with an ultralow interfacial tension of $\gamma_{l_1l_2}$ = 30 μJ/m^2 results in the formation of a spheroid in the DEX drop, whereas increase in the interfacial tension to $\gamma_{l_1l_2}$ = 93 μJ/m^2 disrupts spheroid formation due to the tendency of cells to partition to the interface and the PEG phase. (c) Reproducibility of spheroid formation using the 5.0% PEG−6.4% DEX system in a 96-well plate. The dashed line shows the average diameter of spheroids.

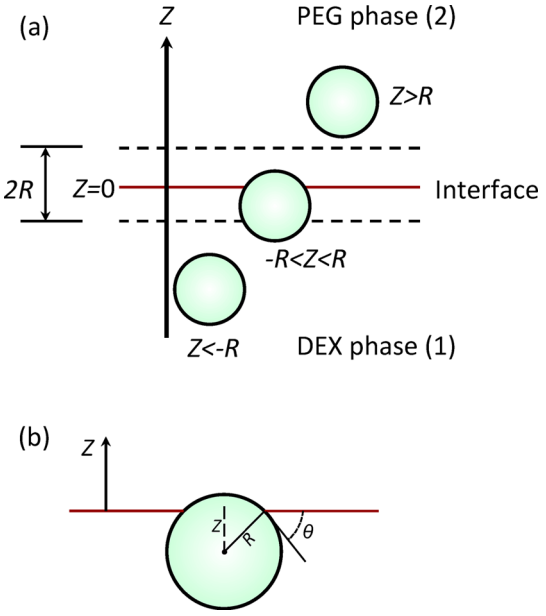

Figure 5. (a) Schematic of model for particle displacement in two-phase systems and (b) contact angle, θ, formed between the particle surface at the interface of two aqueous phases. The thickness of the interface is inversely proportional to the interfacial tension. For the ultralow interfacial tensions measured in this study, the interfacial thickness is small enough that the contact angles are sufficiently well-defined and the model is valid for the reported range of interfacial tensions.

from a practical standpoint, using ATPS of PEG and DEX with low interfacial tensions of ~30 μJ/m^2 is crucial to consistently generate cancer cell spheroids.

Theoretical Model of Cell Partition. To understand the effect of interfacial tension on partition of cells in ATPS, we developed a theoretical model to determine free energy of displacement of cells between the two aqueous phases and their interface (Figure 5a). The approach is based on a model of colloids in a liquid-fluid system.[44] Each cell was considered as a spherical particle of 10 μm radius. We recognize the complexity of the surface of cells compared to colloids. However, the model presented below uses the *measured* values of interfacial tensions of the complex fluid (ATPS) and *measured* contact angles of the ATPS interface against the *actual* cell surface. Therefore, these quantities encode the chemistry of the solutions and surface of cells. We next developed a model of the insertion process that includes the gradient of free energy $U(z)$, which represents the force that the interface asserts in the partition dynamics.

The dynamics of particle transport can be studied through a mesoscopic model in the form of a stochastic partial differential equation, the Langevin equation, which presents a reasonable model of colloid systems with particle sizes above a nanometer scale:[45]

$$d\vec{v}_i = -\zeta_i \vec{v}_i dt + \sum_{j=1}^{N} \vec{F}_{ij} dt - \nabla U_{P_i} dt + V_{P_i}(\rho_{P_i} - \rho_f) g\hat{n} dt + \vec{w}(dt) \quad (2)$$

Here, the velocity of the ith particle is $\vec{v}_i$, and $d\vec{x}_i = \vec{v}_i dt$ obtains; the location of the particle is also stochastic. The friction coefficient is $\xi_i = 6\pi\eta_i R_i$, where η_i is the viscosity of a phase containing the ith particle and R_i is the radius of that particle. The force between particles i and j is $\vec{F}_{ij}$ so that the force field $\sum_{j=1}^{N} \vec{F}_{ij}$ sums over all pairs of particles within a cutoff radius, which determines N. The gradient of the potential $U_{P_i}(Z)$ of particle P_i due to the wetting properties of the solutions provides a force in addition to particle−particle interactions. The effect of gravity is represented by the standard formula wherein V_{P_i} is the volume of particle i, $\rho_{P_i} - \rho_f$ is the density difference between particle i and the fluid surrounding it, g is the acceleration of gravity along the normal to the interface, $\hat{n}$. The last term $\vec{w}(dt)$ is stochastic for which a distribution function, often assumed to be Gaussian and time stationary, and a correlation function (e.g., delta function correlated) must be satisfied. The orders of magnitude of the various terms in eq 2 are relevant. For example, from our analysis above and Figure 3, the effect of gravity on partition of cells in ATPS can be ignored as a small contribution to the Brownian dynamics as compared to other terms.

To understand the importance of particle−particle interactions $\vec{F}_{ij}$, we approximated an average interparticle distance in a dispersion from $L = N_0^{-1/3}$, where N_0 is the number density of cell particles.[46] Using $N_0 = 6 \times 10^6$ cells/mL from our experiments gives an average interparticle spacing of 55 μm between cells dispersed in ATPS during the partition process. This spacing is much greater than the distance at which interparticle interactions (electrostatic and van der Waals) between cells would be important.[47,48] Therefore, the effect of $\vec{F}_{ij}$ can be safely ignored. This conclusion is further supported by findings of Albertsson et al. that partition of cells in ATPS is

DOI: 10.1021/acsami.5b05757
ACS Appl. Mater. Interfaces 2015, 7, 21305−21314

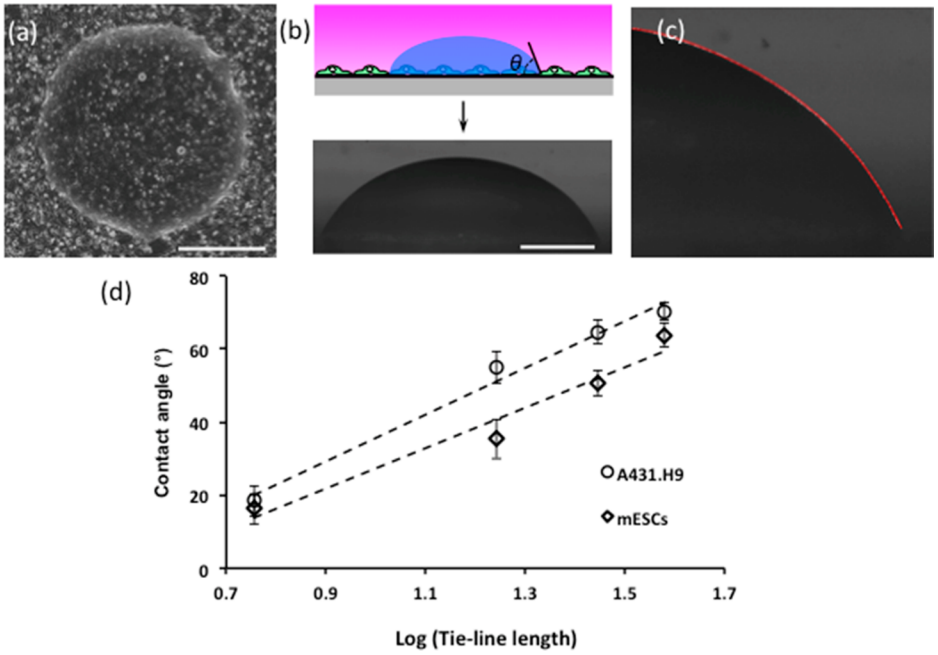

Figure 6. (a) Top view of a sessile drop of ATPS formed on a confluent monolayer of cells, (b) schematic and side view image of a sessile drop of ATPS on a layer of cells, (c) a third-order polynomial fitted to the right side of the drop in panel (b) shown by a red line, and (d) contact angles measured with two-phase systems on A431.H9 cells and mESCs increase with the TLL, in %(w/w), of the two-phase systems shown on a logarithmic scale (base 10). Results indicate that mESCs have a more hydrophilic surface compared to A431.H9. Scale bar is 500 μm.

independent of cell density between 2×10^6 and 1×10^8 cells/mL,[49] a range in which our cell density falls. In addition, we ignore the first term in the equation due to very slow movement of cell particles in the partition process.

This analysis supports our hypothesis that interfacial forces dominate partition of cells in ATPS, at least for the cell−ATPS systems studied here. The effect of interfacial forces can be studied using the model shown in Figure 5. To capture the effect of ultralow interfacial tensions on the partition of cell particles, the theoretical model requires the geometry of particles, the interfacial tension of separation medium, and surface properties of particles characterized through contact angles. Initially, the cell particle was assumed to locate in an arbitrary position Z_0 in the bottom phase (1). Displacement of the particle toward the interface and the top phase (2) was traced using a vector Z perpendicular to the interface. Changes in the free energy associated with displacing the particle from the initial position (Z_0) in the bottom phase to a final arbitrary position (Z) is

$$\Delta U(Z) = \gamma_{l_1l_2}(A_{l_1l_2}(Z) - A_0) + \gamma_{Pl_2}A_{Pl_2}(Z) + \gamma_{Pl1}(A_{Pl_1}(Z) - A_p) \quad (3)$$

where $\gamma_{l_1l_2}$ represents interfacial tension between the two liquid phases, γ_{Pl_1} is the cell-bottom phase interfacial tension, and γ_{Pl_2} denotes the cell-top phase interfacial tension. $A_{l_1l_2}(Z)$ represents the area of liquid−liquid interface when the particle is at a position $-R < Z < R$, A_0 is the total area of interface with a length L and width W, A_{Pl_1} and A_{Pl_2} represent the areas of particle in contact with bottom and top phases, respectively, and A_P denotes surface area of the particle. Using these definitions, we can write

$$A_{Pl_2}(Z) + A_{Pl_1}(Z) = A_p = 4\pi R^2 \quad (4)$$

$$A_{l_1l_2}(Z) + A^p_{l_1l_2}(Z) = A_0 = LW \quad (5)$$

Here, $A^p_{l_1l_2}$ denotes the area of the interface between two liquid phases occupied by the particle. Assuming the validity of Young's equation[50]

$$\gamma_{l_1l_2} \cos \theta_c = \gamma_{Pl_2} - \gamma_{Pl_1} \quad (6)$$

and considering eqs 4 and 5, the free energy eq 3 reduces to

$$\Delta U(Z) = \begin{cases} 0, & Z < -R \\ \gamma_{l_1l_2}[\cos\theta_c A_{Pl_2}(Z) - A^p_{l_1l_2}], & -R < Z < R \\ \gamma_{l_1l_2} \cos\theta_c A_P, & Z > R \end{cases} \quad (7)$$

To evaluate the free energy changes of particle displacement from Z_0 to Z, the interfacial tension between the two aqueous phases (Figure 1) and the contact angle formed on the surface of the particle at the interface of the two phases (Figure 5b) is required.

We developed an alternative method for the determination of contact angles at the interface of the two aqueous phases and a single cell shown in Figure 5b schematic. A monolayer of A431.H9 cells or mESCs was immersed in the aqueous PEG phase. Then a drop of the aqueous DEX phase was dispensed on cells. A typical sessile drop of the DEX phase on cells immersed in the PEG phase is shown in Figure 6a. To estimate contact angles of ATPS drops, we first captured side view images of ATPS drops (Figure 6b). Then we used an automated polynomial fitting technique that uses a standard Canny edge detection method to extract the drop profile and fit a polynomial to each half of the drop profile (Figure 6c).[29] Contact angle was computed as the tangent to the polynomial at the surface. The contact angle of each drop was determined as the average of right and left contact angles. This process was

DOI: 10.1021/acsami.5b05757
ACS Appl. Mater. Interfaces 2015, 7, 21305−21314

repeated for five drops to determine an average contact angle with each two-phase system on cells (Figure 6d). With both cell types, increase in contact angles correlates with the increase in the TLL. With all four systems, a smaller contact angle was measured on mESCs indicating that these cells have a more hydrophilic surface compared to A431.H9 cells. In addition, despite a significant difference in the interfacial tensions of the last three systems, measured contact angles only showed a modest increase. We ensured the validity of these data by contact angle measurements with these four two-phase systems on a bare glass substrate that resulted in a similar trend in contact angles (Figure SI-2).

Next, changes in free energy for cell displacement in each of the two-phase solutions (ΔU) were calculated from eq 7 and plotted versus the position vector Z in Figure 7. Below, results are discussed for each of the two cell types.

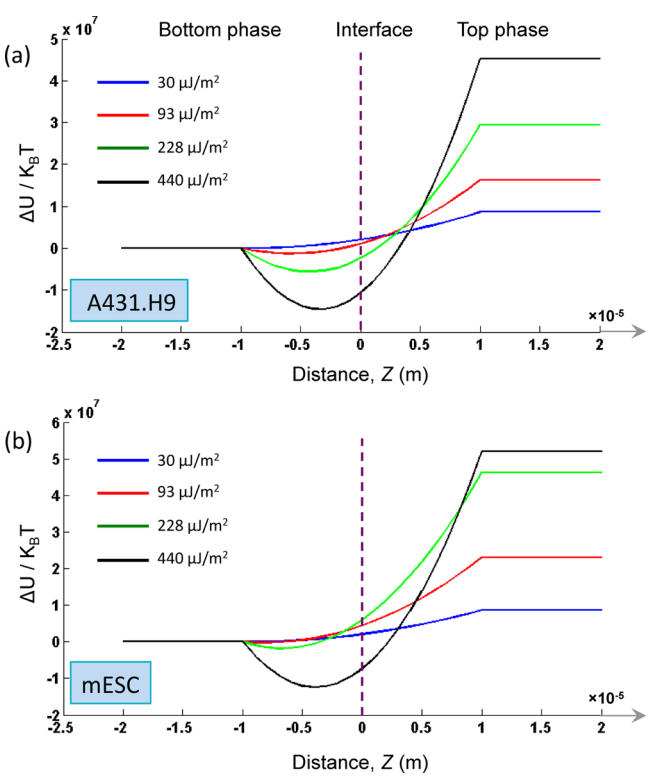

Figure 7. Variations in the free energy associated with displacing a cell particle of 10 μm radius in four two-phase systems calculated based on the theoretical model of eq 7 and measured ultralow interfacial tensions of ATPS and contact angles at the interface of two aqueous phases measured with (a) A431.H9 cancer cells and (b) mESCs. Colors represent these four systems of different interfacial tensions shown in the legend. Free energy is scaled to $K_BT = 4.142 \times 10^{-21}$ J at $T = 300$ K. The dashed line shows the location of the interface. This model predicts partition of cells to a specific phase or interface based on minimum free energy.

The A431.H9 cells (Figure 7a): With the first system that has the smallest interfacial tension of 30 μJ/m^2, the minimum energy happens when the particle locates in the bottom phase. Displacing the particle from its initial position to the interface or the top phase will increase the energy. Therefore, the particle tends to partition to the bottom phase that is energetically favored. Experimentally, cells primarily partitioned to the bottom phase of this two-phase solution and showed a large partition coefficient of 88% (Figure 2c), consistent with the modeling prediction. For the system with an interfacial tension of 93 μJ/m^2, the minimum energy corresponds to the interface and toward the bottom phase, increasing the propensity of particle entrapment at the interface. This is in agreement with the experimental results that showed a significant increase in the partition of cells to the interface in this two-phase solution (Figure 2c), and a decrease of the partition coefficient to 34%. With the two systems with larger interfacial tensions of 226 and 440 μJ/m^2, the minimum energy happened at the interface of the two phases. Experimentally, the partition coefficient in these systems dropped to only 24%. However, the number of cells entrapped at the interface remained more or less constant, but more cells partitioned to the top phase.

The mESCs (Figure 7b): Modeling the partition behavior based on properties of mESCs shows that with the system of $\gamma_{l_1l_2} = 30$ μJ/m^2, the minimum free energy occurs when the particle is in the bottom phase. This reasonably correlates with the experimental partition coefficient of 58% (Figure 2d). With the second system, the minimum energy level is identical when the particle locates in the bottom phase and the interface. Experimentally, this was associated with an increase in the number of cells partitioned to the interface, and over 77% of cells were found at the interface and bottom phase of this system (Figure 2d). With increase in $\gamma_{l_1l_2}$ to 226 μJ/m^2, interfacial cell partition results in minimum free energy. Compared to the second two-phase system, the number of cells at the interface doubled and increased to 59%. The minimum energy is still obtained with the particle partitioning to the interface of the system with $\gamma_{l_1l_2} = 440$ μJ/m^2. This is in a reasonable agreement with our measurements showing that 63% of cells collected at the interface and that the remaining distributed between the top and bottom phases.

Although the largest partition coefficient for both cell types was obtained with the system of $\gamma_{l_1l_2} = 30$ μJ/m^2, mESCs showed a partition coefficient 30% smaller than that of A431.H9 cells in this system. It appears that a very small interfacial tension primes cells to partition to the bottom phase of ATPS, but other factors further affect this process.[26] For example, our contact angle measurements showed that mESCs have a more hydrophilic surface than A431.H9 (Figure 6d). Considering Young's eq 6 provides a plausible explanation: The interfacial tension has a constant value of 30 μJ/m^2 in the first two-phase system. A smaller contact angle with mESCs will cause an increase in the left-hand side of the Young equation. This increase must be balanced by an increase in the difference $\gamma_{pl_2} - \gamma_{pl_1}$, where l_2 and l_1 denote aqueous PEG and DEX phases, respectively. This implies stronger interactions between the aqueous PEG phase and mESCs, compared to the aqueous PEG phase–A431.H9 cells interactions. As a result, a more even distribution of mESCs between aqueous PEG and DEX phases of this two-phase system is expected. This conclusion is consistent with experimental cell partition data (cf. Figure 2c,d).

In addition, examining the free energy curves for displacement of A431.H9 cells in the two-phase systems (Figure 7c) shows a shift in minimum free energy from cells partitioned to the bottom phase of the first system to cells partitioned to the interface of the second system. This explains the significant increase of 44% in the partition of A431.H9 cells to the interface when comparing these two systems. With mESCs, this minimum free energy shift is observed from the second to the

DOI: 10.1021/acsami.5b05757
ACS Appl. Mater. Interfaces 2015, 7, 21305–21314

third system (Figure 7d), elucidating the 53% increase in the number of cells partitioned to the interface.

Overall, this thermodynamic model utilized experimental values reflecting the properties of polymeric aqueous phases and cells to provide a fundamental understanding of the interfacial tension effect on cell partition in aqueous two-phase systems.

CONCLUSIONS

We presented an experimental study of partition of cells in polymeric aqueous two-phase systems (ATPS) and demonstrated that interfacial tension between the equilibrated phases plays a major role on distribution of A431.H9 cancer cells and mESCs between the two phases and their interface. With PEG and DEX of specific properties used as phase-forming polymers, an interfacial tension of 30 $\mu J/m^2$ resulted in the partition of cells primarily to the bottom phase. In this two-phase system, partition of cancer cells to the bottom phase was more significant compared to mESCs. Increasing the interfacial tension through systematic increase in the concentration of polymers shifted cells more toward the interface. A validation study was conducted to demonstrate that a very small interfacial tension was crucial for successful formation of a compact spheroid of cancer cells in the bottom phase drop immersed in the top phase solution. To fundamentally understand this phenomenon, we developed a thermodynamic model to predict free energy changes associated with displacement of cell particles in a two-phase system. This theoretical model suggested that in the system with the smallest interfacial tension of 30 $\mu J/m^2$, the free energy was a minimum when the particle located in the bottom phase. With an increase in the interfacial tension, the minimum free energy state shifted toward the interface, increasing the propensity for cell particles to partition to the interface, corroborating with our experimental observations with two different types of cells. Our data suggested that the shift in cell partition to the interface depended on surface properties of cells. With more hydrophilic mESCs, this occurred at larger interfacial tensions. Future developments of this experimental and theoretical study will provide a more complete picture of cell partition in ATPS by considering the influence of other factors including a diverse set of cells with different size and surface properties and at different stages of cell cycle, molecular weights of polymers, ionic composition of aqueous phases, and temperature and pH of separation medium.

ASSOCIATED CONTENT

Supporting Information

The Supporting Information is available free of charge on the ACS Publications website at DOI: 10.1021/acsami.5b05757.

Phase diagram of the PEG 35k–DEX 500k, plot of contact angles of two-phase systems on bare glass slides. (PDF)

AUTHOR INFORMATION

Corresponding Author

*Phone: 330-972-6031. Fax: 330-374-8834. E-mail: tavana@uakron.edu.

Notes

The authors declare no competing financial interest.

ACKNOWLEDGMENTS

This work is supported by a grant from the NIH (R21CA182333).

REFERENCES

(1) Albertsson, P.-A. *Partition of Cell Particles and Macromolecules,* 3rd ed.; Wiley-Interscience: New York, 1986.

(2) Ferreira, L.; Fan, X.; Mikheeva, L. M.; Madeira, P. P.; Kurgan, L.; Uversky, V. N.; Zaslavsky, B. Y. Structural Features Important for Differences in Protein Partitioning in Aqueous Dextran-Polyethylene Glycol Two-Phase Systems of Different Ionic Compositions. *Biochim. Biophys. Acta, Proteins Proteomics* **2014**, *1844* (3), 694–704.

(3) Muller, W. Separation of Proteins and Nucleic Acids. *Methods Enzymol.* **1994**, *228*, 193–206.

(4) Long, M. S.; Cans, A. S.; Keating, C. D. Budding and Asymmetric Protein Microcompartmentation in Giant Vesicles Containing Two Aqueous Phases. *J. Am. Chem. Soc.* **2008**, *130* (2), 756–762.

(5) Kang, E.-C.; Miyahara, T.; Akiyoshi, K.; Sunamoto, J. Partitioning of Ganglioside-Reconstituted Liposomes in Aqueous Two-Phase Systems. *J. Bioact. Compat. Polym.* **2002**, *17*, 87–104.

(6) Larsson, C.; Sommarin, M.; Widell, S. Isolation of Highly Purified Plant Plasma Membranes and Separation of Inside-Out and Right-Side-Out Vesicles. *Methods Enzymol.* **1994**, *228*, 451–469.

(7) Umakoshi, H.; Kuboi, R.; Komasawa, I. Control of Partitioning of Bacterial Cells and Characterization of Their Surface Properties in Aqueous Two-Phase Systems. *J. Ferment. Bioeng.* **1997**, *84*, 572–578.

(8) Yaguchi, T.; Dwidar, M.; Byun, C. K.; Leung, B.; Lee, S.; Cho, Y. K.; Mitchell, R. J.; Takayama, S. Aqueous Two-Phase System-Derived Biofilms for Bacterial Interaction Studies. *Biomacromolecules* **2012**, *13* (9), 2655–2661.

(9) Hann, S. D.; Goulian, M.; Lee, D.; Stebe, K. J. Trapping and Assembly of Living Colloids at Water–Water Interfaces. *Soft Matter* **2015**, *11*, 1733–1738.

(10) Albertsson, P. A.; Frick, G. Partition of Virus Particles in a Liquid Two-Phase System. *Biochim. Biophys. Acta* **1960**, *37*, 230–237.

(11) Hammar, L.; Eriksson, S.; Malm, K.; Morein, B. Concentration and Purification of Feline Leukaemia Virus (FeLV) and Its Outer Envelope Protein gp70 by Aqueous Two-Phase Systems. *J. Virol. Methods* **1989**, *24* (1–2), 91–101.

(12) Tavana, H.; Jovic, A.; Mosadegh, B.; Lee, Q. Y.; Liu, X.; Luker, K. E.; Luker, G. D.; Weiss, S. J.; Takayama, S. Nanolitre Liquid Patterning in Aqueous Environments for Spatially Defined Reagent Delivery to Mammalian Cells. *Nat. Mater.* **2009**, *8* (9), 736–741.

(13) Soohoo, J. R.; Walker, G. M. Microfluidic Aqueous Two Phase System for Leukocyte Concentration from Whole Blood. *Biomed. Microdevices* **2009**, *11* (2), 323–329.

(14) Vijayakumar, K.; Gulati, S.; de Mello, A. J.; Edel, J. B. Rapid Cell Extraction in Aqueous Two-Phase Microdroplet Systems. *Chem. Sci.* **2010**, *1*, 447–452.

(15) Mace, C. R.; Akbulut, O.; Kumar, A. A.; Shapiro, N. D.; Derda, R.; Patton, M. R.; Whitesides, G. M. Aqueous Multiphase Systems of Polymers and Surfactants Provide Self-Assembling Step-Gradients in Density. *J. Am. Chem. Soc.* **2012**, *134* (22), 9094–9097.

(16) Akbulut, O.; Mace, C. R.; Martinez, R. V.; Kumar, A. A.; Nie, Z.; Patton, M. R.; Whitesides, G. M. Separation of Nanoparticles in Aqueous Multiphase Systems Through Centrifugation. *Nano Lett.* **2012**, *12* (8), 4060–4.

(17) Diamond, A. D.; Hsu, J. T. Protein Partitioning in PEG/DEX Aqueous Two-Phase Systems. *AIChE J.* **1990**, *36*, 1017–1024.

(18) Tavana, H.; Mosadegh, B.; Takayama, S. Polymeric Aqueous Biphasic Systems for Non-Contact Cell Printing on Cells: Engineering Heterocellular Embryonic Stem Cell Niches. *Adv. Mater.* **2010**, *22* (24), 2628–2631.

(19) Tavana, H.; Mosadegh, B.; Zamankhan, P.; Grotberg, J. B.; Takayama, S. Microprinted Feeder Cells Guide Embryonic Stem Cell Fate. *Biotechnol. Bioeng.* **2011**, *108*, 2509–2516.

DOI: 10.1021/acsami.5b05757
ACS Appl. Mater. Interfaces 2015, 7, 21305–21314

(20) Atefi, E.; Lemmo, S.; Fyffe, D.; Luker, G. D.; Tavana, H. High Throughput, Polymeric Aqueous Two-Phase Printing of Tumor Spheroids. *Adv. Funct. Mater.* **2014**, *24* (41), 6509−6515.
(21) Lemmo, S.; Atefi, E.; Luker, G. D.; Tavana, H. Optimization of Aqueous Biphasic Tumor Spheroid Microtechnology for Anti-Cancer Drug Testing in 3D Culture. *Cell. Mol. Bioeng.* **2014**, *7* (3), 344−354.
(22) Lemmo, S.; Nasrollahi, S.; Tavana, H. Aqueous Biphasic Cancer Cell Migration Assay Enables Robust, High-Throughput Screening of Anti-Cancer Compounds. *Biotechnol. J.* **2014**, *9*, 426−434.
(23) Tavana, H.; Kaylan, K.; Bersano-Begey, T.; Luker, K. E.; Luker, G. D.; Takayama, S. Polymeric Aqueous Biphasic System Rehydration Facilitates High Throughput Cell Exclusion Patterning for Cell Migration Studies. *Adv. Funct. Mater.* **2011**, *21* (15), 2920−2926.
(24) Ham, S. L.; Nasrollahi, S.; Shah, K. N.; Soltisz, A.; Paruchuri, S.; Yun, Y. H.; Luker, G. D.; Bishayee, A.; Tavana, H. Phytochemicals Potently Inhibit Migration of Metastatic Breast Cancer Cells. *Integr Biol.* **2015**, *7* (7), 792−800.
(25) Frampton, J. P.; Leung, B. M.; Bingham, E. L.; Lesher-Perez, S. C.; Wang, J. D.; Sarhan, H. T.; El-Sayed, M. E. H.; Feinberg, S. E.; Takayama, S. Rapid Self-Assembly of Macroscale Tissue Constructs at Biphasic Aqueous Interfaces. *Adv. Funct. Mater.* **2015**, *25*, 1694−1699.
(26) Cabral, J. M. Cell Partitioning in Aqueous Two-Phase Polymer Systems. *Adv. Biochem Eng. Biotechnol* **2008**, *106*, 151−171.
(27) Atefi, E.; Mann, J. A., Jr.; Tavana, H. Ultralow Interfacial Tensions of Aqueous Two-Phase Systems Measured Using Drop Shape. *Langmuir* **2014**, *30* (32), 9691−9.
(28) Lahooti, S.; del Rio, O.; Cheng, P.; Neumann, A. W. Axisymmetric Drop Shape Analysis (ADSA). In *Applied Surface Thermodynamics;* Neumann, A. W., Spelt, J. K., Eds.; Marcel Dekker: New York, 1996; Chapter 10, pp 441−507.
(29) Atefi, E.; Mann, J. A., Jr.; Tavana, H. A Robust Polynomial Fitting Approach for Contact Angle Measurements. *Langmuir* **2013**, *29* (19), 5677−88.
(30) Ham, S. L.; Atefi, E.; Fyffe, D.; Tavana, H. Robotic Production of Cancer Cell Spheroids with an Aqueous Two-Phase System for Drug Testing. *J. Visualized Exp.* **2015**, *98*, e52754.
(31) Albertsson, P. A.; Tjerneld, F. Phase Diagrams. *Methods Enzymol.* **1994**, *228*, 3−13.
(32) Alanazi, I.; Ebrahimie, E.; Hoffmann, P.; Adelson, D. L. Combined Gene expression and Proteomic Analysis of EGF Induced Apoptosis in A431 Cells Suggests Multiple Pathways Trigger Apoptosis. *Apoptosis* **2013**, *18* (11), 1291−305.
(33) Gatti, L.; Beretta, G. L.; Carenini, N.; Corna, E.; Zunino, F.; Perego, P. Gene Expression Profiles in the Cellular Response to a Multinuclear Platinum Complex. *Cell. Mol. Life Sci.* **2004**, *61* (7−8), 973−81.
(34) Ginis, I.; Luo, Y.; Miura, T.; Thies, S.; Brandenberger, R.; Gerecht-Nir, S.; Amit, M.; Hoke, A.; Carpenter, M. K.; Itskovitz-Eldor, J.; Rao, M. S. Differences Between Human and Mouse Embryonic Stem Cells. *Dev. Biol.* **2004**, *269*, 360−380.
(35) Palmqvist, L.; Glover, C. H.; Hsu, L.; Lu, M.; Bossen, B.; Piret, J. M.; Humphries, R. K.; Helgason, C. D. Correlation of Murine Embryonic Stem Cell Gene Expression Profiles with Functional Measures of Pluripotency. *Stem Cells* **2005**, *23* (5), 663−80.
(36) Sainz, J.; Garcia-Alcalde, F.; Blanco, A.; Concha, A. Genome-Wide Gene Expression Analysis in Mouse Embryonic Stem Cells. *Int. J. Dev. Biol.* **2011**, *55* (10−12), 995−1006.
(37) Raymond, F. D.; Fisher, D. Partition of Rat Erythrocytes in Aqueous Polymer Two Phase Systems. *Biochim. Biophys. Acta, Biomembr.* **1980**, *596*, 445−450.
(38) Godin, M.; Bryan, A. K.; Burg, T.; Babcock, K.; Manalis, S. R. Measuring the Mass, Density and Size of Particles and Cells Using a Suspended Microchannel Resonator. *Appl. Phys. Lett.* **2007**, *91*, 123121.
(39) Grover, W. H.; Bryan, A. K.; Diez-Silva, M.; Suresh, S.; Higgins, J. M.; Manalis, S. R. Measuring Single-Cell Density. *Proc. Natl. Acad. Sci. U. S. A.* **2011**, *108* (27), 10992−6.
(40) Gerson, D. F. Cell Surface Energy, Contact Angles and Phase Separation. *Biochim. Biophys. Acta, Biomembr.* **1980**, *602*, 269−280.
(41) Reid, B. G.; Jerjian, T.; Patel, P.; Zhou, Q.; Yoo, B. H.; Kabos, P.; Sartorius, C. A.; Labarbera, D. V. Live Multicellular Tumor Spheroid Models for High-Content Imaging and Screening in Cancer Drug Discovery. *Curr. Chem. Genomics Transl. Med.* **2014**, *8*, 27−35.
(42) Thoma, C. R.; Zimmermann, M.; Agarkova, I.; Kelm, J. M.; Krek, W. 3D Cell Culture Systems Modeling Tumor Growth Determinants in Cancer Target Discovery. *Adv. Drug Delivery Rev.* **2014**, *69*−*70*, 29−41.
(43) Carver, K.; Ming, X.; Juliano, R. L. Multicellular Tumor Spheroids as a Model for Assessing Delivery of Oligonucleotides in Three Dimensions. *Mol. Ther.–Nucleic Acids* **2014**, *3*, e153.
(44) Pieranski, P. Two-Dimensional Interfacial Colloidal Crystals. *Phys. Rev. Lett.* **1980**, *45*, 569−572.
(45) Reichl, L. E. *A Modern Course in Statistical Physics,* 2nd ed.; Wiley: New York, 1998.
(46) Kryuchkov, Y. N. Concentration Dependence of the Mean Distance Between Particles in Disperse Systems. *Refract. Ind. Ceram.* **2001**, *42*, 390−392.
(47) Israelachvili, J. N. *Intermolecular and Surface Forces,* 3rd ed.; Academic Press: 2011.
(48) Bowen, W. R.; Sharif, A. O. Long-Range Electrostatic Attraction Between Like-Charge Spheres in a Charged Pore. *Nature* **1998**, *393*, 663−665.
(49) Albertsson, P. A.; Baird, G. D. Counter-Current Distribution of Cells. *Exp. Cell Res.* **1962**, *28*, 296−322.
(50) Young, T. An Essay on the Cohesion of Fluids. *Philos. Trans R Soc. Lnd* **1805**, *95*, 65−87.

DOI: 10.1021/acsami.5b05757
ACS Appl. Mater. Interfaces 2015, 7, 21305−21314